Available online at www.sciencedirect.com
SCIENCE DIRECT®
Bioorganic & Medicinal Chemistry 12 (2004) 5973–5982
Bioorganic & Medicinal Chemistry

Catalytic transformations with copper-metalated diglycine conjugates

C. Madhavaiah,[a] Masood Parvez[b] and Sandeep Verma[a,*]

[a]*Department of Chemistry, Indian Institute of Technology-Kanpur, Kanpur 208016, India*
[b]*Department of Chemistry, The University of Calgary, 2500 University Drive NW, Calgary, Canada T2N1N4*

Received 3 August 2004; accepted 12 August 2004
Available online 11 September 2004

Abstract—A series of copper-metalated, water-soluble bis-diglycine conjugates were synthesized and characterized through spectroscopic methods. These conjugates were evaluated for the cleavage of phosphodiester substrates, supercoiled plasmid relaxation in the presence of co-oxidants, and for the oxidation of a diphenolic substrate, 2,6-dimethoxyphenol. Appreciable rate enhancements were observed for these reactions and the oxidative nucleolytic cleavage activity and phenol oxidative coupling was presumably manifested via formation of reactive oxygen species.

1. Introduction

Metal ions are essential structural and functional co-factors for enzymatic transformations, where they either activate reactants or stabilize intermediates/transition states, *en route* to catalysis. Modeling of metal-binding sites in proteins has enhanced our understanding of the role of metal ions in catalytic reactions and has led to novel design paradigms for crafting metal-binding motifs for various applications.[1]

Amino terminal Cu(II) and Ni(II) binding motif (ATCUN), found in serum albumin, is implicated for the transport of metal ions and small molecules.[2] This motif is present in human, bovine, and rat serum albumin, neuromedins C and K, human sperm protamine P2a, and histatins. The crystal structure of tripeptide (Cu-GGH-N-methyl amide) indicate that the metal ion is tetra-coordinated with the participation of amino terminal of nitrogen, two deprotonated peptide nitrogens, and histidyl imidazole nitrogen, in a slightly distorted square planar arrangement.

Pauling and co-workers reported antitumor activity of Cu-GGH motif in the presence of ascorbate, presumably through the generation of reactive oxygen species.[3] Since then, several reports have described transformation of DNA binding proteins to site specific artificial nucleases by the tethering them to the Cu-GGH motif.[4] Amino acid substitutions have also been utilized to generate structure–activity relationship to include other amino acids in tripeptide variants.[5] In addition to nuclease activity, this motif was used to accomplish protein cross-linking and to probe protein–protein interactions, in the presence of co-oxidants and metal co-factors.[6]

We have previously reported phosphatase and nuclease activity of *insoluble*, dipeptide conjugates.[7] These constructs were rendered insoluble for heterogeneous catalysis through deliberate molecular design and a novel feature of reusability of metal–peptide complex was described by us.[7c] Herein, we present synthesis, crystal structure analysis, characterization of copper complexes and catalytic activities of soluble diglycine conjugates and probable mechanism of oxidative nucleic acid cleavage and phenol oxidative coupling by these complexes.

2. Results and discussions

2.1. Synthesis and characterization

Soluble diglycine conjugates were prepared by reacting *N*-hydroxysuccinamide ester of *Boc*-protected diglycine with a variety of diaminoalkanes such as, 1,2-diaminoethane, 1,3-diaminopropane, 1,4-diaminobutane,

Keywords: Diglycine; Copper; Catalysis; Plasmid; Oxidation.
* Corresponding author. Tel.: +91 512 2597643; fax: +91 512 2597436; e-mail: sverma@iitk.ac.in

0968-0896/$ - see front matter © 2004 Elsevier Ltd. All rights reserved.
doi:10.1016/j.bmc.2004.08.018

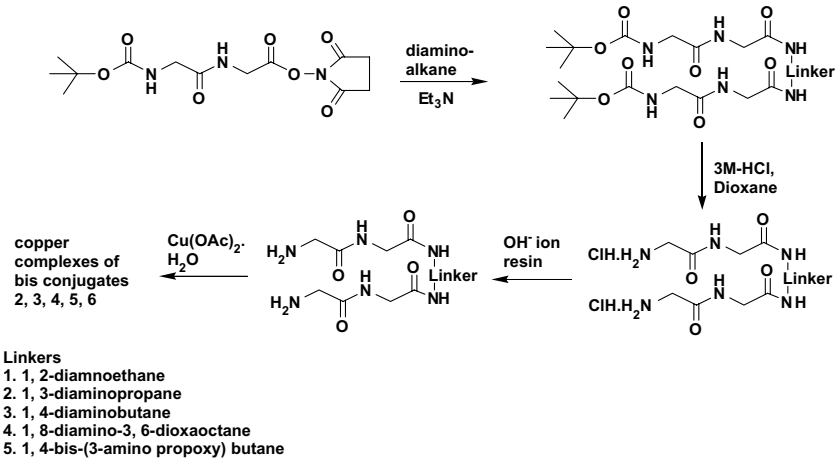

Scheme 1. Synthesis of copper metalated bis-diglycine conjugates **2**–**6**.

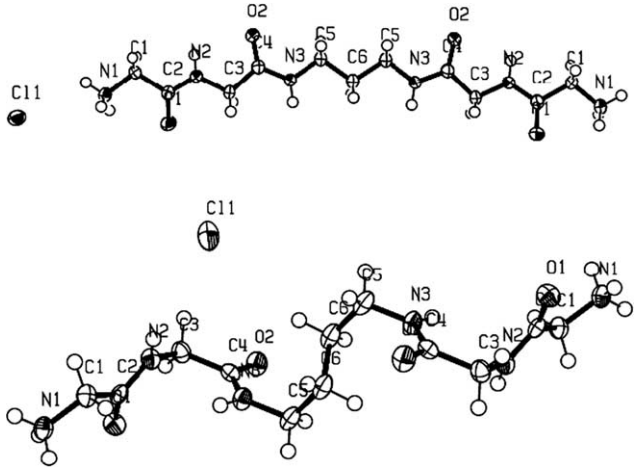

Figure 1. ORTEP diagram of conjugate 3 and 4 contains Cl^- ion.

1,8-di- amino-3,6-dioxaoctane, and 1,4-bis-(3-amino-propoxy)- butane. *t*-Boc group was deprotected with 3 M HCl-dioxane, followed by anion exchange resin treatment, to afford diglycine conjugates (Scheme 1).

These were characterized spectroscopically and single crystal X-ray structure was determined for two constructs (Fig. 1).[†] As expected, extended hydrogen bonding was observed in both crystal structures, via the participation of backbone –NH, –C=O, and Cl^- ions (Fig. 2a and b).

The presence of a chloride ion in the unit cell of **3** enables formation of a weak hydrogen bond corresponding to C(5)–H(5)···Cl(1), with a 2.75 Å length and an angle of 165.12°. While in conjugate **4**, C–H···Cl interactions with two different carbons were observed. These are C(1)–H(1)···Cl(1) with 2.78 Å length, with a corresponding angle 143.42°. The other one, C(3)–H(3)···Cl(1), displayed 2.64 Å length, with a corresponding angle of 144.23°. Apart from these nonconventional interactions, conventional interactions stabilize the crystal structure with a slight hint of helicity being imparted to **4**, perhaps due to a longer aliphatic linker length. Important hydrogen bond lengths and bond angles are mentioned in Table 1.

We were unable to grow crystals of metalated diglycine conjugates, therefore we resorted to mass spectroscopy in order to characterize the pattern of copper coordination in these conjugates. Soft ionizing-desorption techniques, such as ESI-MS, allow for facile transfer and detection of intact metalated species. This technique is frequently used to provide accurate mass assignments for metal (copper) complexes by deciphering stoichiometric speciation.[8] Consequently, ESI mass spectra was recorded for metalated conjugates **2**–**6** and monocopper and dicopper fragments and possible molecular ions peaks were assigned (Table 2).

The mass spectrum for **4** is shown in Figure 3 and its analysis is described. For this complex, *m*/*z* value 378 suggests for the existence of monocopper species and a low abundance *m*/*z* value 439 indicates the presence of dicopper species with four deprotonated nitrogens. Dimeric species containing monocopper and dicopper centers were also observed at *m*/*z* values of 755 and 878, respectively. Dicopper center, with one acetate ligand, three deprotonated peptide nitrogens was observed at 499 and the corresponding dimer was observed at 999. A peak with *m*/*z* value 682 was identified as possible molecular ion, comprising of two copper ions, *probably* coordinated to four acetates, terminal amino nitrogen and amide carbonyl. Proposed ESI mass fragmentation pattern of conjugate **4** is detailed in Scheme 2. Importantly, peaks corresponding to three or more copper ions in the complex were negligible. The stoichiometry was further confirmed by determining copper in metalated conjugates by atomic absorption spectroscopic analysis, which revealed for the presence of 2 copper ions/ligand for all diglycine conjugates (data not shown).

[†] Crystallographic data (excluding structure factors) for the structures **3**, **4** have been deposited with Cambridge Crystallographic Data Center. CCDC number for **3** is 234717 and for **4** CCDC number is 234718.

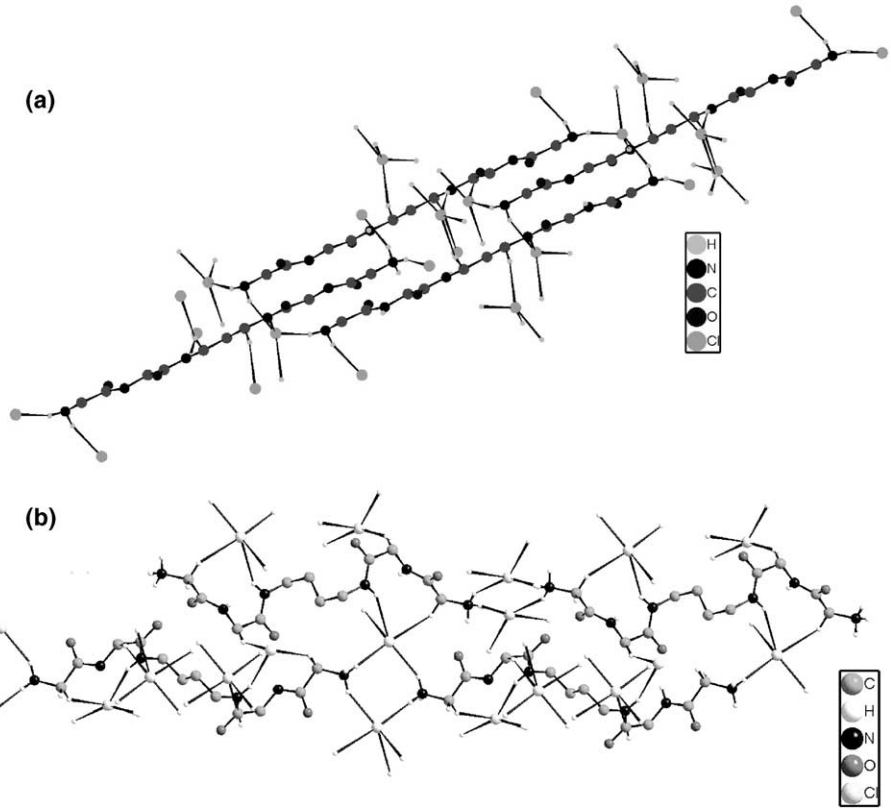

Figure 2. (a, b) Diamond 2.1, rendered stacking diagram of conjugate **3**, and **4** hydrogen atoms were excluded for the clarity.

Table 1. Bond lengths (Å) and bond angles (°) for the conjugates **3** and **4**

D–H···A	*d*(D–H)	*d*(H···A)	<(DHA)
For conjugate **3**[a]			
N(1)–H(1A)···O(2) #1	0.91	1.99	168
N(1)–H(1B)···Cl(1) #2	0.91	2.28	157
N(1)–H(1C)···Cl(1) #3	0.91	2.25	158
N(2)–H(2)···O(2) #4	0.88	2.29	150
N(2)–H(2)···O(1) #5	0.88	2.58	116
N(3)–H(3)···Cl(1) #6	0.88	2.40	160
C(5_2)–H(5b)···Cl(1) #7	0.99	2.75(17)	165.12
For conjugate **4**[b]			
N(1)–H(1N1)···Cl(1) #1	0.89(2)	2.28(2)	169.2(18)
N(1)–H(2N1)···Cl(1) #2	0.89(2)	2.38(2)	152.1(18)
N(1)–H(3N1)···O(1) #3	0.93(2)	1.90(2)	157.7(18)
N(2)–H(1N2)···O(2) #4	0.88	2.07	165
N(3)–H(1N3)···Cl(1) #5	0.88	2.56	147.7
C(1)–H(1A)···Cl(1) #6	0.99(2)	2.78	143.4(9)
C(3)–H(3A)···Cl(1) #7	0.99(11)	2.64	144.23(11)

[a] Symmetry operations: #1 $-x+1/2, y-1/2, -z+1/2$; #2 $-x+1, -y+1, -z+1$; #3 $-x+1, y, -z+1/2$; #4 $-x+1/2, -y+3/2, -z$; #5 $-x+1/2, y+1/2, -z+1/2$; #6 $x-1/2, -y+1/2, z-1/2$; #7 $-0.5+x, -0.5+y, -1+z$.

[b] Symmetry operations: #1 $-x+1, -y, -z$; #2 $x+1, y, z$; #3 $-x+2, y-1/2, -z+1/2$; #4 $-x+1, y-1/2, -z+1/2$; #5 $-x+1, y-1/2, -z+1/2$; #6 $1-x, -0.5+y, 0.5-z$; #7 x, y, z.

The electronic spectra of all metalated conjugates exhibited λ_{max} at 650 nm. EPR spectra for copper complexes were recorded in methanol, at liquid nitrogen temperature (Fig. 4), and calculated *g* values are presented in Table 3. The *g* values appeared as $g_{\|} > g_{\perp} > 2$, which suggest for a square-based geometry around the copper center.[9] However, the exact geometry of copper in these complexes cannot be confirmed in the absence of X-ray crystal structures.

FT-IR spectroscopy offers potentially useful information about metal peptide interactions. The following general comments can be made about changes in the IR spectra of metalated conjugates vis-à-vis their unmetalated counterparts.

- It is known that shifts in amide I band (C=O str vibrations weakly coupled with C–N str and in-plane N–H bending) frequencies, lying between 1620 and 1625 cm^{-1}, indicates participation of carbonyl group in metal ion coordination.[10] Such shifts, between 1620 and 1627 cm^{-1}, were observed in our complexes thus confirming involvement of carbonyl oxygens in copper coordination (Table 4).
- N–H str frequencies were also shifted to lower energies, while amide II band (in-plane N–H bending strongly coupled to C–N str) was shifted to higher frequency numbers, suggesting for possible involvement of terminal amino groups for copper coordination, as shown in Scheme 2. Such shifts were consistent for a pair of conjugate and its metalated derivative.

2.2. Phosphodiesterase activity of conjugates 2–6

We evaluated these complexes for their assistance in facilitating three different reactions under homogeneous

Table 2. Possible fragments in ESI MS[a] of copper metalated conjugates

Complex	Monocopper fragment	Dicopper center fragment	Possible molecular ion peak
2	350 $[(L+a)-2H]^{+\cdot}$	473 $[(L+2a+b)-H]$	654 $[(L+2a+4b)+3H]^{+\cdot}$
3	364 $[(L+a)-2H]^{+\cdot}$	485 $[(L+2a+b)-3H]^{+\cdot}$	668 $[(L+2a+4b)+3H]^{+\cdot}$
4	378 $[(L+a)-2H]^{+\cdot}$	499 $[(L+2a+b)-3H]^{+\cdot}$	682 $[(L+2a+4b)+3H]^{+\cdot}$
5	438 $[(L+a)-2H]^{+\cdot}$	499 $[(L+2a)-4H]^{+\cdot}$	742 $[(L+2a+4b)+3H]^{+\cdot}$
6	494 $[(L+a)-2H]^{+\cdot}$	557 $[(L+2a)-2H]^{+\cdot}$	798 $[(L+2a+4b)+3H]^{+\cdot}$

[a] All complexes were dissolved in water and were introduced into the ESI source through a syringe pump at the rate of 5 μL/min. The ESI capillary was set at 3.5 kV and the cone voltage was 40 V. The spectra were collected in 6 s scans and the print outs are averaged spectra of 6–8 scans. *L*, *a*, *b* are indicates the molecular weights of unmetalated conjugate, copper (Cu), and acetate (–OAc), respectively. Ligands mol. wt. 302, 316, 376, 432, respectively, for **2**–**6**, while molecular weights were 63.5 and 59, for Cu and –OAc, respectively.

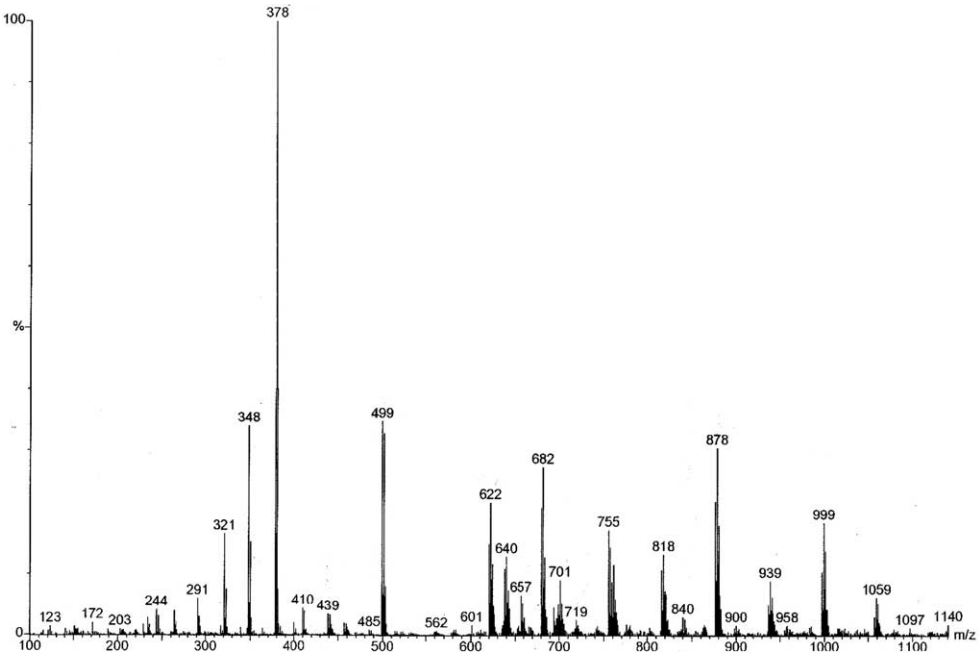

Figure 3. ESI mass spectrum of copper metalated conjugate **4**.

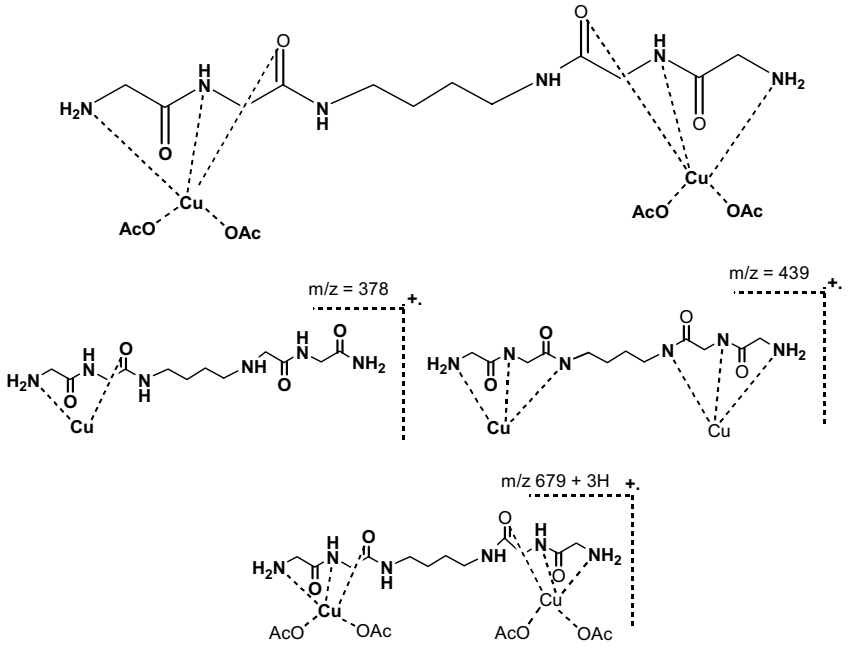

Scheme 2. Possible fragmentation of **4/Cu**, in ESI process.

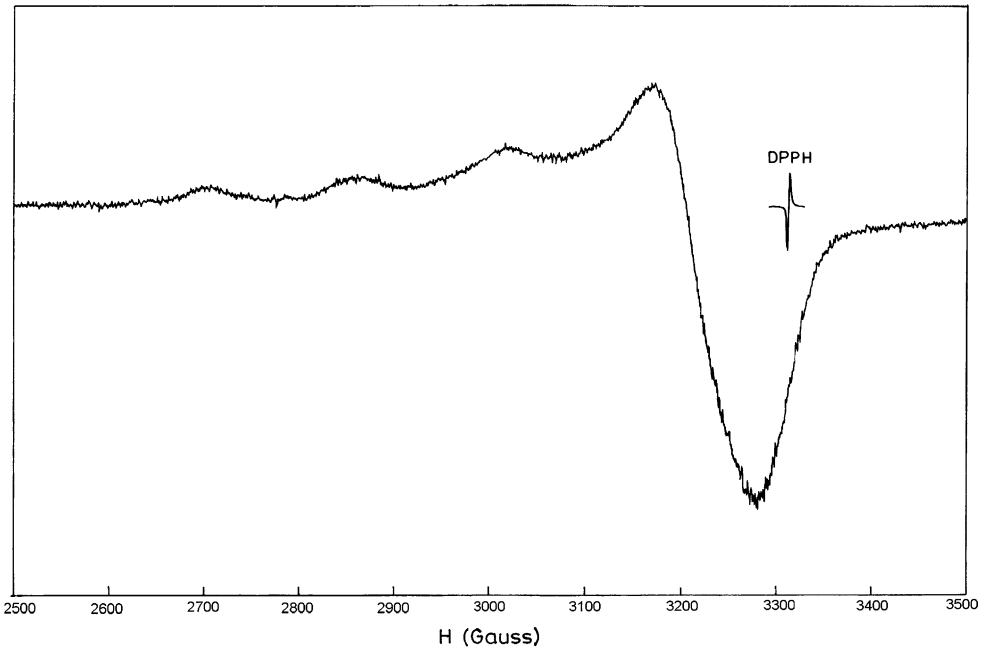

Figure 4. EPR spectra of **4/Cu**.

Table 3. EPR properties of copper metalated conjugates **2**–**6**

Copper complex	$g_{\parallel}$	$g_{\perp}$	$A_{\parallel}$(G)
2	2.286	2.062	142.5
3	2.254	2.052	152.5
4	2.257	2.056	160
5	2.258	2.065	155
6	2.260	2.056	157.5

Table 4. IR (KBr pellet) values of unmetalated and metalated conjugates

Conjugate	Amide I (cm^{-1})	Amide II (cm^{-1})	–NH (str, cm^{-1})
2	1651	1558	3286
2/Cu	1627	1583	3281
3	1642	1545	3295
3/Cu	1627	1581	3272
4	1643	1547	3291
4/Cu	1620	1581	3273
5	1645	1555	3277
5/Cu	1625	1584	3267
6	1645	1549	3285
6/Cu	1620	1585	3267

reaction conditions. Detailed kinetic analysis was performed for the cleavage of two nonnatural phosphodiesters, bNPP and hNPP, in presence of **2**–**6**. Pseudo-first-order rate constants were calculated from $\ln A_{\infty}/A_{\infty} - A_t$ versus time plots. The rate constants and corresponding rate enhancements are mentioned in Table 5. bNPP hydrolysis was accelerated to the tune of 2–5 million fold over the uncatalyzed reaction,[11] which was comparable to reported synthetic phosphodiesterases.[12] Corresponding rate constants for hNPP hydrolysis were also determined and are mentioned in Table 5.

Table 5. Pseudo-first-order rate constants for bNPP and hNPP hydrolysis, catalyzed by complexes **2**–**6**[a]

Substrate	Complex	k_{obs} ($\times 10^{-3}$) (min^{-1})	k_{rel}
bNPP[b]	**2**	1.91	2.45×10^6
	3	1.33	1.70×10^6
	4	2.18	2.80×10^6
	5	1.39	1.78×10^6
	6	3.95	5.06×10^6
hNPP[c]	**2**	1.22	616
	3	1.21	611
	4	1.45	735
	5	0.75	361
	6	2.47	1247

[a] All hydrolytic reactions were performed in duplicate, in 3 mL of 0.01 M of *N*-eththylmorpholine aqueous buffer pH = 8.0, $T = 40\,^{\circ}C$ for bNPP and 30 °C for hNPP hydrolysis. Weight of the catalysts were 1 mg/mL of substrate solution corresponding to the 1.5, 1.49, 1.46, 1.35, 1.25 mM, respectively, for **2**–**6** copper complexes.
[b] Concentration was 12 mM.
[c] Concentration was 4 mM.

A saturation curve was generated for bNPP hydrolysis catalyzed by copper complex **4** displaying a reasonable Michaelis–Menten type behavior (Fig. 5). Detailed kinetic analysis was further performed to derive Michaelis–Menten constant (K_m), turnover number (k_{cat}), and maximal velocities (V_{max}) from corresponding Lineweaver–Burk plots and the values are reported in Table 6.

2.3. pH and solvent effect over bNPP hydrolysis catalyzed by 4/Cu

Pseudo-first-order rate constants for bNPP hydrolysis catalyzed by **4/Cu** were determined for various pH

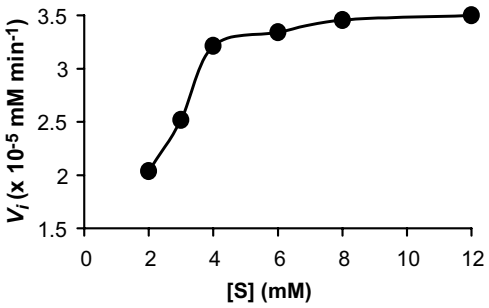

Figure 5. Saturation curve for bNPP hydrolysis catalyzed by **4/Cu**.

Table 6. Michaelis–Menten constants for bNPP and hNPP hydrolysis catalyzed by complexes **2**–**6**[a]

Substrate	Complex	K_m (mM)	V_{max} ($\times 10^{-5}$) (mM min^{-1})	k_{cat} ($\times 10^{-5}$) (min^{-1})
bNPP[b]	**2**	5.14	13.72	9.27
	3	4.45	14.8	10.33
	4	2.77	4.93	3.52
	5	5.08	10.56	18.12
	6	9.78	17.15	13.72
hNPP[c]	**2**	4.98	40.65	27.63
	3	1.43	22.72	15.97
	4	5.14	59.94	39.24
	5	4.81	34.48	26.53
	6	3.74	51.28	41.21

[a] All hydrolytic reactions were performed in duplicate in 3 mL of 0.01 M of *N*-ethylmorpholine buffer at pH 8, 40 °C for bNPP, 30 °C for hNPP hydrolysis. Weight of the complexes was 1 mg/1 mL of substrate solution, corresponding to 1.5, 1.49, 1.46, 1.35, and 1.25 mM, respectively, for complexes **2**–**6**.
[b] Concentrations range was 3–9 mM.
[c] Concentrations range was 0.25–1 mM.

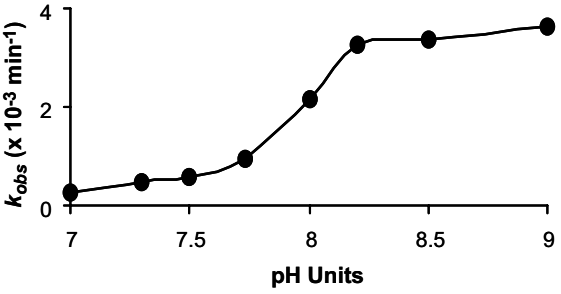

Figure 6. pH curve for bNPP hydrolysis catalyzed by complex **4/Cu**.

values (7–9). Interestingly, catalytic profile was pH-dependent and a sigmoidal curve was obtained (Fig. 6). Such profiles have been reported for other synthetic phosphodiesterases containing transition metal ions and represent a deprotonation event, presumably leading to a hydrolytic pathway.[13] It is established that transition metal ions lower pK_a of metal-bound water leading to the generation of hydoxyl ion, which can act either as a general base to activate solvent water or as a nucleophile to attack at the phosphorous center.

Table 7. Solvent effect over bNPP hydrolysis by **4/Cu**[a]

S. no	Solvent system	k_{obs} ($\times 10^{-3}$) (min^{-1})	k_{rel}
1	Pure ethylene glycol	0.8	1
2	50% ethylene glycol	1.662	2.077
3	Pure water	2.18	2.75

[a] All hydrolytic reactions were performed in duplicate in 0.01 M *N*-ethylmorpholine buffer prepared in respective solvent systems (pH = 8.0, T = 40 °C). Concentration of the substrate was 12 mM and the weight of the catalyst was 1 mg/mL, corresponding to 1.46 mM.

The preference for a solvent system was also ascertained by performing cleavage reactions in water, ethylene glycol, and 50% aqueous ethylene glycol. The rate of the reaction increased from pure ethylene glycol to water suggesting preferential generation of metal-bound hydroxyl ion rather than metal-bound alkoxy ion (Table 7). Differential reactivities of metal-bound hydroxide versus alkoxide ions, by employing an alcohol pendant group have appeared in literature.[14]

2.4. pBR322 supercoiled plasmid relaxation

Metalated ATCUN motif and related peptides cleave DNA in the presence of added co-oxidants.[3,5c–e] Supercoiled pBR322 DNA cleavage was achieved for conjugates **2**–**6**, in the presence of externally added co-oxidant magnesium monoperoxyphthalate. The conversion of form **I** to form **II** by complex **4** occurred rapidly in the presence of MMPP (Fig. 7A, Lane 5). Expectedly, the cleavage reaction was completely inhibited in presence of EDTA, confirming a crucial role of coordinated copper in bis-diglycine conjugates (Fig. 7B, Lane 4).

Plasmid modification was completely inhibited in presence of NaN_3 suggesting a role of oxygen derived reactive species in cleavage reactions (data not shown). Consequently, the role of oxygen was probed by conducting cleavage reactions under anaerobic reaction conditions in a glove-bag. Nearly 50% of the cleavage reaction was quenched, thus emphasizing the need and involvement of oxygen in cleavage reactions (Fig. 7B, Lane 2). Similar cleavage profiles were also observed for other conjugates as well (Fig. 8).

2.5. Phenol oxidation activity of 4/Cu

Polyphenol oxidases (tyrosinases), laccases, and other copper metalloenzymes catalyze oxidative transforma-

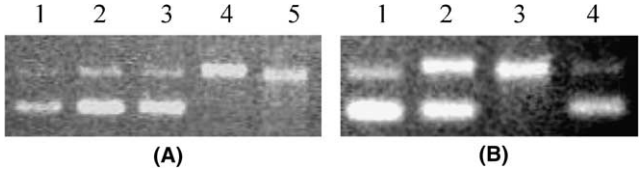

Figure 7. (A) Plasmid relaxation by complex **4**. Lane 1: pBR322 alone; Lane 2: DNA+MMPP (10 min); Lane 3: DNA+**4** (10 min); Lanes 4, 5: pBR322+**4**+MMPP (3, 6 min, respectively). (B) pBR322 cleavage under anaerobic conditions by complex **4**: Lane 1: pBR322 alone; Lane 2: pBR322+**4**+MMPP (anaerobic conditions, 8 min); Lane 3: pBR322+**4**+MMPP (8 min); Lane 4: pBR322+**4**+MMPP+EDTA.

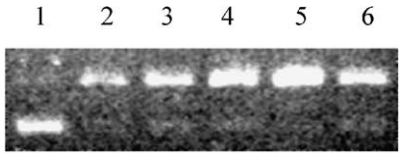

Figure 8. pBR322 cleavage catalyzed by complexes **2**–**6**: Lane 1: pBR322; Lanes 2–6: pBR322+MMPP+complexes **2**–**6**, respectively (8 min).

tion of a variety of natural and nonnatural aromatic compounds.[15] Consequently, design, synthesis, and activities of complexes mimicking precise coordination environment of copper in these enzymes, continues to attract considerable attention.[16]

Although digycline conjugates were not designed for phenol oxidation potential, we thought of investigating this activity for 2,6-dimethoxyphenol (DMP) as substrate, considering facile oxidative nucleic acid cleavage and a body of evidence available for DMP oxidation by mono- and dinuclear copper complexes and also by an oligomeric catalyst.[17] Consequently, **4/Cu** was reacted with DMP, which was used as a monophenolic substrate, in the absence of exogenously added co-oxidants.

DMP is known to react with enzymes and copper complexes to yield the corresponding *para*-coupled diquinone, 2,2′,6,6′-tetramethoxydibenzo-1,1′-diquinone. Co-incubation with H_2O_2 or MMPP, led to the formation of black tar-like product indicating rapid oxidative polymerization of DMP in presence of exogenous oxidants, perhaps due to its higher reactivity compared to plasmid DNA. However, we were able to follow a more controlled reaction by simple incubation of **4/Cu** with DMP (Scheme 3).

Kinetic parameters K_m, V_{max}, and k_{cat} were calculated from corresponding Lineweaver–Burk plot (Fig. 9) and these values were found to be 11.37 mM, 14.4×10^{-3} mM min^{-1}, and 31.8×10^{-3} min^{-1}, respectively. As with DNA cleavage experiment, inhibition of 2,6-DMP oxidation was observed with different concentrations of EDTA. Lineweaver–Burk plot was generated in the presence of 0.05 mM of EDTA. Michaelis–Menten parameters K_m, V_{max} were found to be 4.18 mM, 4.54×10^{-3} mM min^{-1} (Fig. 9), indicating a decelerated reaction. Complete inhibition was observed in presence of 0.5 mM EDTA, which can be attributed to possible complex formation confirming an important role of coordinated copper for oxidative reactions. Unmetalated conjugates did not elicit any activity even

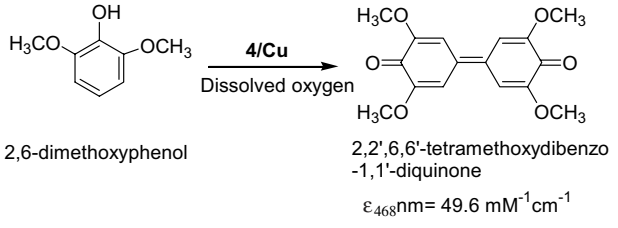

Scheme 3. Oxidation of 2,6-DMP by **4/Cu**.

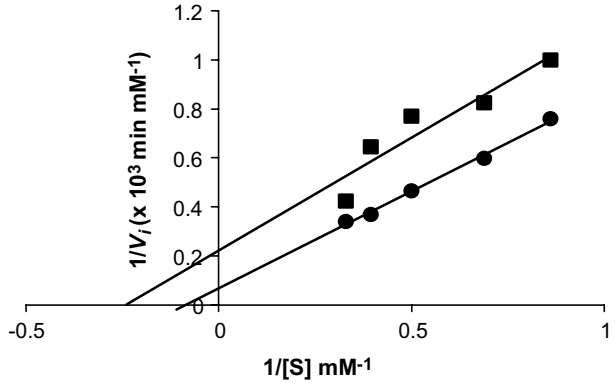

Figure 9. Lineweaver–Burk plot for 2,6-DMP oxidation, catalyzed by **4/Cu**. Without EDTA (●); In presence of 0.05 mM of EDTA (■).

in the presence of exogenous co-oxidants and these co-oxidants alone were also incapable of oxidizing DMP.

The role of dissolved oxygen in aqueous buffer for reaction catalysis was probed by performing oxidation reaction in degassed, freeze-thawed buffer. V_i decreased for degassed buffer suggesting oxygen dependence (data not shown). Although we have not yet studied this effect in detail, preliminary results support a crucial role of dissolved oxygen for oxidation in absence of added H_2O_2 or MMPP. Further experiments are being planned to evaluate oxygen dependence and extending the scope of this oxidation to other relevant substrates.

In conclusion, we have crafted several copper metalated water-soluble bis-diglycine conjugates by deriving inspiration from metal ion-binding GGH motif of serum albumin. Their catalytic assistance toward phosphate ester hydrolysis and DNA cleavage reactions demonstrate that N-terminus histidine in GGH motif is probably not essential for nuclease activity. Using a bioinformatics approach, we have recently reported ATCUN-like metal-binding motif variants in proteins through identification and characterization of crystal structures in databases and by sequence analysis.[18] Oxidation of DMP and corresponding EDTA inhibition was also investigated. Efforts were made to probe mechanistic pathways for supercoiled plasmid modification and phenol oxidation.

3. Experimental section

3.1. Chemicals and reagents

Glycylglycine, *N*,*N*′-dicyclohexylcarbodiimide, copper acetate, and *N*-hydroxysuccinamide were purchased from Lancaster (England). *N*-Hydroxysuccinamide was recrystallized from hot ethyl acetate prior to use. Di *tert*-butyl-dicarbonate, bis-*p*-(nitrophenyl)phosphate (bNPP) were purchased from Fluka (Switzerland), and bNPP was converted to its sodium salt by adjusting pH 7.0 with 1 N NaOH. RNA model substrate, 2-hydroxypropyl-*p*-nitrophenyl phosphate (hNPP) was synthesized using a literature procedure.[19] *tert*-Butyloxycarbonylglycylglycine[20] and the corresponding

N-hydroxysuccinamide ester were prepared according to the literature procedure.[21] 1,2-Dimethoxyethane, triethylamine, and 1,2-diaminoethane (S. D. Fine chemicals, Bombay, India) were dried according to the standard procedures. 1,8-Diamino-3,6-dioxaoctane (Merk, India), and 1,4-bis-(3-aminopropoxy)butane (Fluka, Switzerland) were distilled over potassium hydroxide, prior to use. NMR spectra were recorded using a JEOL 400 MHz spectrometer in d_6-DMSO (Aldrich) or in D_2O. FAB MS and ESI MS were recorded at RSIC, Lucknow and AAS values were recorded at FEAT Laboratory, IIT-Kanpur.

3.2. Synthesis and characterization of bis-diglycine conjugates

3.2.1. 1-Succinimidyl-*N*-*tert*-butyloxycarbonylglycylglycinate (1). To pre-cooled solution of *tert*-butyloxycarbonylglycylglycine (10.53 g, 45 mmol) in dimethoxyethane (40 mL), *N*-hydroxysuccinimide (5.22 g, 45 mmol) and DCC (9.35 g, 45 mmol) were added at 0 °C. Then the reaction mixture was stirred for 2 h at 0 °C then for 12 h at room temperature. After this time the precipitated dicyclohexylurea was filtered and washed with DMF, then evaporated under reduced pressure. The residue was recrystallized from hot isopropyl alcohol to give **1** (12.7 g, yield 85%, mp 159–161 °C).

^{1}H NMR (400 MHz, 25 °C, $CDCl_3$, TMS, δ ppm): 1.45 (s, 9H, *t*-Boc H); 2.847 (s, 4H, succinimidyl ring H), 3.87 (d, $J = 5.6$ Hz, 2H, –Gly H); 4.423 (d, $J = 5.6$ Hz, 2H, –Gly H); 5.287 (br s, 1H, *t*-Boc NH), 6.922 (t, $J = 5.2$ Hz, 1H, –NH).

3.2.2. *N*,*N*′-Bis-(*tert*-butyloxycarbonylglycylglycine)-1,2-diaminoethane (2a). To the mixture of **1** (2.4 g, 7.3 mmol), and triethylamine (1.0 mL, 7.3 mmol) in dry dimethoxyethane (30 mL), 1,2-diaminoethane (0.24 mL, 3.64 mmol) in dimethoxyethane (1 mL), was added drop wise with rigorous stirring. Then stirring was continued for 4 h at room temperature. The precipitated compound was filtered and washed with 1,4-dioxane followed by with cold water and air dried to give pure compound **2a** (1.53 g, yield 86%, mp 200–202 °C). ^{1}H NMR (400 MHz, d_6-DMSO, 25 °C, TMS, δ ppm): 1.3845 (s, 18H, *t*-Boc); 3.110 (br s, 4H, linker's $-CH_2CH_2$); 3.578 (br s, 4H, Gly $-CH_2$); 3.751 (br s, 4H, Gly $-CH_2$); 7.026 (br s, 2H, –NH); 7.861 (br s, 2H, –NH); 8.035 (br s, 2H, –NH); FAB MS (M+1) = 489.

3.2.3. *N*,*N*′-Bis-(glycylglycine)-1,2-diaminoethane (2). Compound **2a** (1.48 g, 3.03 mmol) was stirred with 3 M HCl-dioxane (17 mL) for 4 h at room temperature. After this time solvent was evaporated and the residue was washed with methanol (5 × 10 mL), and then followed by acetone (3 × 10 mL) and air dried to give **2** (1.07 g, yield 98%, mp 234–236 °C), as its hydrochloride. This hydrochloride salt was dissolved in double distilled water and passed through strong anion exchange resin. The water was evaporated and the residue was washed with methanol, followed by acetone to give **2** (0.8 g, yield 93%, mp 198–200 °C). ^{1}H NMR (400 MHz, D_2O, 25 °C, δ ppm): 3.36 (s, 4H, linker's $-CH_2CH_2$); 3.41 (s, 4H, Gly $-CH_2$); 3.924 (s, 4H, Gly $-CH_2$); ^{13}C (100 MHz, D_2O, 25 °C) δ 39.387, 43.105, 44.504, 172.6, 177.125; FT IR (KBr, cm^{-1}) = 1558 (amide II, –NH def); 1651 (amide I, –C=O str); 3286 (–NH str); FAB MS (M+1) = 289.

3.2.4. *N*,*N*′-Bis-(*tert*-butyloxycarbonylglycylglycine)-1,3-diaminopropane (3a). To the solution of **1** (1.2 g, 3.64 mmol) in dimethoxyethane (20 mL), 1,3-diaminopropane (0.15 mL, 1.82 mmol) in dimethoxyethane (0.5 mL) was added drop wise with constant stirring. Then stirring was continued for 4 h, a precipitate so formed was filtered and washed with 1,4-dioxane followed by acetone to give **3a** (0.49 g, yield 53%, mp 143–145 °C). ^{1}H NMR (400 MHz, d_6-DMSO, 25 °C, TMS, δ ppm): 1.386 (s, 18H, *t*-Boc); 1.525 (t, $J = 6.8$ Hz, 2H, linker's $-CH_2CH_2$); 3.058 (q, $J = 6.8$ Hz, 4H, linker's $-NHCH_2$); 3.548 (d, $J = 5.6$ Hz, 4H, Gly CH_2); 3.657 (d, 5.6 Hz, 4H, Gly CH_2); 7.017 (t, $J = 5.6$ Hz, 2H, –NH); 7.754 (t, $J = 5.16$ Hz, 2H, –NH); 8.039 (t, $J = 5.6$ Hz, 2H, –NH); ^{13}C NMR (100 MHz, d_6-DMSO, 25 °C, TMS, δ ppm): 28.18, 29.15, 36.24, 42.05, 43.40, 78.18, 155.91, 168.70, 169.70; FAB MS (M+1): 503.

3.2.5. *N*,*N*′-Bis-(glycylglycine)-1,3-diaminopropane (3). Compound **3a** (1.17 g, 2.33 mmol), was treated with 3 M HCl-dioxane (12 mL) for 4 h, at room temperature with constant stirring. Then the solvent was evaporated and the residue was washed with methanol (3 × 10 mL) followed by acetone (3 × 10 mL) and the compound was air dried to give **5** as its hydrochloride salt (0.83 g, yield 95%, mp 241–243 °C). This hydrochloride salt was passed through strong anion exchange resin. After evaporation of water, the compound was washed with methanol, followed by acetone to give of **3** (0.65 g, yield 96%, mp 177–179 °C). ^{1}H NMR (400 MHz, D_2O, 25 °C, TMS, δ ppm): 1.710 (t, $J = 7.2$ Hz, 2H, linkers $-CH_2$); 3.238 (t, $J = 6.8$ Hz, 4H, linker's $-NHCH_2$); 3.417 (s, 4H, Gly $-CH_2$); 3.925 (s, 4H, Gly $-CH_2$); ^{13}C NMR (100 MHz, D_2O, 25 °C, TMS, δ ppm): 28.64, 37.2, 43.19, 44.48, 172.21, 171.14; FT IR (KBr, cm^{-1}) = 1545 (amide II, –NH def); 1642 (amide I, –C=O str); 3295 (–NH str); FAB MS (M+1) = 303.

3.2.6. *N*,*N*′-Bis-(*tert*-butyloxycarbonylglycylglycine)-1,4-diaminobutane (4a). To the compound **1** (1.26 g, 3.8 mmol) in dimethoxyethane (20 mL), triethylamine (0.53 mL, 3.8 mmol) was added. To this 1,4-diaminobutane (0.19 mL, 1.9 mmol) in dimethoxyethane (0.5 mL) was added drop wise with rigorous stirring. Then stirring was continued for 4 h, a white precipitate so formed was filtered and washed with cold water and then 1,4-dioxane, followed by acetone, air dried to give **4a** (0.76 g, yield was 77%, mp 174–176 °C). ^{1}H NMR (400 MHz, d_6-DMSO, 25 °C, TMS, δ ppm): 1.384 (br s, 22H, overlapped signal for *t*-Boc and linker's $-CH_2$); 3.039 (br s, 4H, linker's $-CH_2NH$); 3.55 (d, $J = 5.2$ Hz, 4H, Gly $-CH_2$); 3.651 (d, $J = 4.8$ Hz, 4H, Gly $-CH_2$); 7.039 (t, $J = 5.6$ Hz, 2H, –NH); 7.234 (t, $J = 5.2$ Hz, 2H, –NH); 8.012 (t, $J = 5.68$ Hz, 2H, –NH); FAB MS (M+1): 517.

3.2.7. *N,N′*-Bis-(glycylglycine)-1,4-diaminobutane (4). Compound **4a** (2.2 g, 4.25 mmol) was treated with 3 M HCl-dioxane (30 mL) for 4 h at room temperature with constant stirring. After this time solvent was evaporated and the residue was washed with methanol (3 × 10 mL), followed by acetone (3 × 10 mL), then the compound was air dried to give **4** as its hydrochloride (1.3 g, yield 80%, mp 218–220 °C). This hydrochloride (0.85 g, 2.18 mmol) was passed through strong anion exchange resin and evaporated the water, to give **4**. This compound was washed with methanol followed by acetone to give pure **4** (0.675 g, yield 98%, mp 188–190 °C). ^{1}H NMR (400 MHz, D_2O, 25 °C, TMS, δ ppm): 1.508 (br s, 4H, linker's $-CH_2CH_2$); 3.224 (br s, 4H, linker's $-NHCH_2$), 3.406 (s, 4H, Gly $-CH_2$); 3.914 (s, 4H, Gly $-CH_2$); ^{13}C NMR (100 MHz, D_2O, 25 °C, δ ppm): 26.56, 38.22, 41.79, 44.634, 168.625, 173.07; FT IR (KBr, cm^{-1}): 1547 (amide II, –NH def); 1644 (amide I, –C=O str); 3292 (–NH str); FAB MS (M+1): 317.

3.2.8. *N,N′*-Bis-(glycylglycine)-1,8-diamino-3,6-dioxaoctane (5). To the solution of **1** (1 g, 3.0 mmol) in dimethoxyethane (14 mL), 1,8-diamino-3,6-dioxaoctane (0.22 mL, 1.52 mmol) in dimethoxyethane (0.5 mL) was added drop wise with constant stirring. After 2 h stirring at room temperature, solvent was evaporated, and the crude compound was treated with 3 M HCl-1,4-dioxane (8 mL) for 3 h. Then the solvent was evaporated, and residue was triturated with 1:1 mixture of acetone and methanol at 0 °C, to give **5** as its hydrochloride salt (0.5 g, yield was 73%). This hydrochloride salt (0.88 g, 0.8 mmol) was passed through strong basic anion exchange resin to give of *N,N′*-bis-(glycylglycine)-1,8-diamino-3,6-dioxaoctane (0.3 g, yield 93%, mp 137–139 °C). ^{1}H NMR (400 MHz, D_2O, 25 °C, δ ppm): 3.290 (t, $J = 5$ Hz, 4H, linker's $-NHCH_2$), 3.493 (t, $J = 5$ Hz, 4H, linker's $-CH_2O$); 3.539 (s, 4H, linker's $-OCH_2CH_2O-$); 3.755 (s, 4H, Gly $-CH_2$), 3.846 (s, 4H, Gly $-CH_2$); ^{13}C NMR (100 MHz, D_2O, 25 °C, δ ppm): 39.68, 41.20, 43.09, 69.514, 70.164, 168.50, 171.91; FT IR (KBr, cm^{-1}): 1556 (amide II, –NH def); 1645 (amide I, –C=O str); 3277 (–NH str); FAB MS (M+1): 377.

3.2.9. *N,N′*-Bis-(glycylglycine)-1,4-bis-(3-aminopropoxy)butane (6). To the solution of **1** (1.36 g, 4.1 mmol) in dimethoxyethane (18 mL), 1,4-bis-(3-aminopropoxy)butane (0.44 mL, 2.06 mol) in dimethoxyethane (0.5 mL) was added drop wise with constant stirring. After 2 h stirring at room temperature, solvent was evaporated, and the crude compound was treated with 3 M HCl-1,4-dioxane (15 mL) for 3 h. Then the solvent was evaporated, and residue was washed with 1:1 mixture of acetone and methanol at 0 °C, to give **6** as its hydrochloride salt (0.9 g, yield 86%). This hydrochloride salt (0.527 g, 0.1 mmol) was passed through strong anion resin to give **6** (0.42 g, yield 93%, mp 133–135 °C). ^{1}H NMR (400 MHz, D_2O, 25 °C, δ ppm): 1.482 (br s, 4H, linker's $-CH_2CH_2O$); 1.651 (q, $J = 6.8$ Hz, 4H, linker's $-OCH_2CH_2$); 3.151 (t, $J = 6.8$ Hz, 4H, linker's $-NHCH_2$); 3.399 (br t, 4H, overlapped signals for linker's $-CH_2OCH_2$); 3.764 (s, 4H, Gly $-CH_2$); 3.826 (s, 4H, Gly $-CH_2$); ^{13}C NMR (100 MHz, D_2O, 25 °C, δ ppm): 26.11, 29.07, 37.26, 41.25, 43.20, 68.59, 71.18, 168.511, 171.671; FT IR (KBr, cm^{-1}): 1549 (amide II, –NH def); 1645 (amide I, –C=O str); 3295 (–NH str); FAB MS (M+1): 433.

3.2.10. Anion exchange column. Strong anion exchange resin (Dowex 1-X8) was washed with three column volumes (3 × 30 mL) of 0.5 N NaOH prepared in 80% of aqueous dioxane, followed by three column volumes of 0.1 N NaOH. Then the column was washed with water until the washings showed the neutral pH (pH 7.0). Then the hydrochloride salts of conjugates were dissolved in water and passed through the column. The column was washed with water, washings are combined and evaporated to give corresponding conjugates as its free amines.

3.2.11. Metalation of bis-diglycine conjugates. Conjugates **2**, **3**, **4**, **5**, **6** were metalated with 2 equiv of copper acetate monohydrate, in aqueous methanol. After 5 h stirring at room temperature, solvent was evaporated, residue was triturated with acetone, 1,4-dioxane, finally with acetone. The blue compound so obtained was dried in vacuum, and characterized by using EPR, AAS, EI MS, UV–vis spectroscopy, and IR. The amount of copper incorporated was determined by using atomic absorption spectroscopy. These values are compared with spectrophotometric method. Then the resulted copper complexes were used for phosphate ester hydrolysis, DNA cleavage reactions.

3.3. General procedure for kinetic experiments

3.3.1. Phosphate ester hydrolysis. All hydrolytic reactions were performed in duplicate in centrifuge tubes thermostated at 40 °C for bNPP hydrolysis or at 30 °C for hNPP hydrolysis. The assay mixture contained 3 mL of substrate solution of appropriate concentration prepared in 0.01 M *N*-ethylmorpholine (NEM) aqueous buffer at pH 8.0, unless otherwise mentioned. The reference cell contained substrate without metal conjugates, to correct for background hydrolysis. Final concentrations of metalated conjugates **2**–**6** were 1.48, 1.42, 1.4, 1.3, and 1.25 mM, respectively. Control experiments proved that incubation of unmetalated peptide conjugates and copper acetate alone, with phosphate ester substrates, did not accelerate hydrolysis. Initial velocities were determined as a function of time-dependent release of *p*-nitrophenolate anion ($\varepsilon_{400} = 1.65 \times 10^4$ M^{-1}cm^{-1}), with a Shimadzu UV-160 spectrophotometer. Michaelis–Menten parameters were determined using corresponding Lineweaver–Burk plots, while the pseudo-first-order rate constants were derived from $\ln A_\infty/A_\infty - A_t$ versus time plots. All hydrolytic reactions were performed at least over five half-lives of each substrate.

3.3.2. pBR322 cleavage experiment. All cleavage reactions were performed in cacodylate buffer (10 mM, pH 7.5), at 35 °C, unless otherwise mentioned. Total reaction volume was 20 μL and weight of the DNA was 8 ng/μL of buffer. Final concentration of conjugates and MMPP were 100 μM. For scavenger gel experiment weight of the DNA was 7 ng/μL of buffer, and

concentrations of conjugates, MMPP were 100 μM. All reactions were quenched with 5 μL of loading buffer contains 100 mM of EDTA, 50% glycerol in Tris–Hcl, pH 8.0 and the samples were loaded onto 0.7% of agarose gel containing ethidium bromide (1 μg/mL). Finally gels were imaged on PC-interfaced Bio-Rad Gel Documentation System 2000.

3.4. Oxidative coupling of 2,6-dimethoxyphenol

Oxidative reactions were performed in 1.5 mL of UV-cuvettes in 0.01 M of *N*-ethylmorpholine buffer (pH 7.5, 30 °C) and total reaction volume was 1.2 mL. Reference cell contained substrate without **4/Cu**. The concentration of **4/Cu** was taken, as 0.5 mM and substrate concentration range was 1–3 mM for the generation of Lineweaver–Burk plot. The progress of the reaction was monitored spectrophotometrically by time dependent formation of 2,2′,6,6′-tetramethoxydibenzo-1,1′-diquinone at 468 nm ($\varepsilon = 49.6\,mM^{-1}cm^{-1}$).[22]

3.4.1. Anaerobic-reaction. The cacodylate buffer was purged with nitrogen gas followed by subjecting to four freeze-thaw cycles. Transfer of reagents and cleavage reactions were performed in argon filled glove bag. Quenching of the reactions was done by addition of loading buffer in the argon filled glove bag.

Acknowledgements

C.M. thanks Council for Scientific and Industrial Research (CSIR) for award of a SRF. This work was partially supported by funds from the Department of Science and Technology, India, to one of us (S.V.).

References and notes

1. (a) Xing, G.; DeRose, V. J. *Curr. Opin. Chem. Biol.* **2001**, *5*, 196; (b) DeGrado, W. F.; Summa, C. M.; Pavone, V.; Nastri, F.; Lombardi, A. *Annu. Rev. Biochem.* **1999**, *68*, 779.
2. Harford, C.; Sarkar, B. *Acc. Chem. Res.* **1997**, *30*, 123.
3. (a) Kimoto, E.; Tanaka, H.; Gyotoku, J.; Morishige, F.; Pauling, L. *Cancer Res.* **1983**, *43*, 824; (b) Chiou, S. H. *J. Biochem.* (*Tokyo*) **1983**, *94*, 1259.
4. (a) Mack, D. P.; Iverson, B. L.; Dervan, P. B. *J. Am. Chem. Soc.* **1988**, *110*, 7572; (b) Mack, D. P.; Dervan, P. B. *J. Am. Chem. Soc.* **1990**, *112*, 4604; (c) Mack, D. P.; Dervan, P. B. *Biochemistry* **1992**, *31*, 9399; (d) Harford, C.; Narindrasorasak, S.; Sarkar, B. *Biochemistry* **1996**, *35*, 4271; (e) Footer, M.; Egholm, M.; Kron, S.; Coull, J. M.; Matsudaria, P. *Biochemistry* **1996**, *35*, 10673.
5. (a) Shullenberger, D. F.; Eason, P. D.; Long, E. C. *J. Am. Chem. Soc.* **1993**, *115*, 11038; (b) Muller, J. G.; Hickerson, R. P.; Perez, J. R.; Burrows, C. J. *J. Am. Chem. Soc.* **1997**, *119*, 1501; (c) Qi, L.; Ananias, D. C.; Long, E. C. *J. Am. Chem. Soc.* **1998**, *120*, 248; (d) Huang, X.; Pieczko, M. E.; Long, E. C. *Biochemistry* **1999**, *38*, 2160; (e) Nagane, R.; Koshigoe, T.; Chikira, M. *J. Inorg. Biochem.* **2003**, *93*, 204.
6. (a) Brown, K. C.; Yang, S. H.; Kodadek, T. *Biochemistry* **1995**, *34*, 4733; (b) Bertrand, R.; Derancourt, J.; Kassab, R. *Biochemistry* **1997**, *36*, 9703; (c) Brown, K. C.; Yu, Z.; Burlingame, A. S.; Craik, C. S. *Biochemistry* **1998**, *37*, 4397; (d) Mal, T. K.; Ikura, M.; Kay, L. E. *J. Am. Chem. Soc.* **2002**, *124*, 14002.
7. (a) Madhavaiah, C.; Verma, S. *Bioconjugate Chem.* **2001**, *12*, 855; (b) Madhavaiah, C.; Verma, S. *Bioorg. Med. Chem. Lett.* **2003**, *13*, 923; (c) Madhavaiah, C.; Srivatsan, S. G.; Verma, S. *Catal. Commun.* **2003**, *4*, 237.
8. (a) Brown, D. R.; Guantieri, V.; Grasso, G.; Impellizzeri, G.; Pappalardo, G.; Rizzarelli, E. *J. Inorg. Biochem.* **2004**, *98*, 133; (b) Colette, S.; Amekraz, B.; Madic, C.; Berthon, L.; Cote, G.; Moulin, C. *Inorg. Chem.* **2003**, *42*, 2215; (c) Whittal, R. M.; Ball, H. L.; Cohen, F. E.; Burlingame, A. L.; Prusiner, S. B.; Baldwin, M. A. *Protein Sci.* **2000**, *9*, 332; (d) Wan, K. X.; Shibue, T.; Gross, M. L. *J. Am. Chem. Soc.* **2000**, *122*, 300.
9. Vaidyanathan, M.; Balamurugan, R.; Sivagnanam, U.; Palaniandavar, M. *J. Chem. Soc., Dalton Trans.* **2001**, 3498.
10. Facchini, G.; Torre, M. H.; Kremer, E.; Piro, O. E.; Castellano, E. E.; Baran, E. J. *J. Inorg. Biochem.* **2002**, *89*, 174, and references cited therein.
11. (a) Breslow, R.; Huang, D.-L. *Proc. Natl. Acad. Sci. U.S.A.* **1991**, *88*, 4080; (b) Vance, D. H.; Czarnik, A. W. *J. Am. Chem. Soc.* **1993**, *115*, 12165.
12. (a) Srivatsan, S. G.; Verma, S. *Chem. Eur. J.* **2002**, *8*, 5184; (b) Srivatsan, S. G.; Verma, S. *Chem. Eur. J.* **2001**, *7*, 828; (c) Vance, D. H.; Czarnik, A. W. *J. Am. Chem. Soc.* **1993**, *115*, 12165; (d) Moss, R. A.; Bracken, K.; Zhang, J. *Chem. Commun.* **1997**, 563.
13. (a) Raivji, G. H.; Milburn, R. M. *Inorg. Chim. Acta* **1988**, *150*, 227; (b) Kady, I. O.; Tan, B.; Ho, Z.; Scarborough, T. *J. Chem. Soc., Chem. Commun.* **1995**, 1137; (c) Deal, K. A.; Burstyn, J. N. *Inorg. Chem.* **1996**, *35*, 2792.
14. Young, M. J.; Wahnon, D.; Hynes, R. C.; Chin, J. *J. Am. Chem. Soc.* **1995**, *117*, 9441.
15. (a) Solano, F.; Lucas-Elio, P.; Lopez-Serrano, D.; Fernandez, E.; Sanchez-Amat, A. *FEMS Microbiol. Lett.* **2001**, *204*, 175; (b) Johannes, C.; Majcherczyk, A. *J. Biotech.* **2000**, *78*, 193; (c) Youn, H. D.; Hah, Y. C.; Kang, S. *FEMS Microbiol. Lett.* **1995**, *132*, 183; (d) Yaropolov, A. I.; Skorobogatko, O. V.; Vartanov, S. S.; Varfolomeyev, S. D. *Appl. Biochem. Biotechnol.* **1994**, *49*, 257; (e) Pandey, G.; Muralikrishna, C.; Bhalerao, U. T. *Tetrahedron Lett.* **1990**, *31*, 3771.
16. Lewis, E. A.; Tolman, W. B. *Chem. Rev.* **2004**, *104*, 1047.
17. (a) Nishino, H.; Satoh, H.; Yamashita, M.; Kurosawa, K. *J. Chem. Soc., Perkin Trans. 2* **1999**, 1919; (b) Rockcliffe, D. A.; Martell, A. E. *J. Mol. Catal. A* **1996**, *106*, 211; (c) Maruyama, K.; Tsukube, H.; Araki, T. *Chem. Lett.* **1979**, 499.
18. Sankararamakrishnan, R.; Verma, S.; Kumar, S. *Proteins: Struct. Funct. Bioinformatics*, in press.
19. Brown, D. M.; Usher, D. A. *J. Chem. Soc.* **1965**, 6558.
20. Ponnusamy, E.; Fotadar, U.; Spisni, A.; Fiat, D. *Synthesis* **1986**, 48.
21. Salvadori, S.; Menegatti, E.; Sarto, G.; Tomatis, R. *J. Pept. Protein Res.* **1981**, *18*, 393.
22. Wariishi, H.; Vallis, K.; Gold, M. H. *J. Biol. Chem.* **1992**, *267*, 23688.